Front. Mater. Sci. 2011, 5(3): 301–310
DOI 10.1007/s11706-011-0142-4

RESEARCH ARTICLE

In vivo bone regeneration with injectable chitosan/hydroxyapatite/collagen composites and mesenchymal stem cells

Zhi HUANG[1], Yan CHEN*[2], Qing-Ling FENG (✉)[1], Wei ZHAO[3], Bo YU (✉)[4], Jing TIAN[4], Song-Jian LI[4], and Bo-Miao LIN[5]

1 Department of Materials Science and Engineering, Tsinghua University, Beijing 100084, China
2 Department of Ultrasonic Diagnosis, Zhujiang Hospital of Southern Medical University, Guangzhou 510282, China
3 Institute of High Energy Physics, Chinese Academy of Sciences, Beijing 100049, China
4 Department of Orthopedics, Zhujiang Hospital of Southern Medical University, Guangzhou 510282, China
5 Department of Radiology, Zhujiang Hospital of Southern Medical University, Guangzhou 510282, China

ABSTRACT: For reconstruction of irregular bone defects, injectable biomaterials are more appropriate than the preformed biomaterials. We herein develop a biomimetic *in situ*-forming composite consisting of chitosan (CS) and mineralized collagen fibrils (nHAC), which has a complex hierarchical structure similar to natural bone. The CS/nHAC composites with or without mesenchymal stem cells (MSCs) are injected into cancellous bone defects at the distal end of rabbit femurs. Defects are assessed by radiographic, histological diagnosis and Raman microscopy until 12 weeks. The results show that MSCs improve the biocompatibility of CS/nHAC composites and enhance new bone formation *in vivo* at 12 weeks. It can be concluded that the injectable CS/nHAC composites combined with MSCs may be a novel method for reconstruction of irregular bone defects.

KEYWORDS: mineralized collagen fibrils, *in situ*-forming, injectable, mesenchymal stem cells, tissue engineered bone

1 Introduction

For reconstruction of irregular bone defects following the surgical removal of cysts or tumours, injectable scaffolds is more appropriate than the preformed scaffolds [1]. In the case of the preformed scaffolds, prior knowledge of the size and shape of irregular defects or cavity are problematical [2]; however, injectable scaffolds, particularly those delivered in aqueous solution, can fill irregular bone defects with minimally invasive surgery and are considered ideal delivery vehicles for cells [3].

A chitosan/glycerophosphate salt formulation was prepared as a biocompatible injectable vehicle for mesenchymal stem cells (MSCs) delivery [4]. Chitosan (CS) is a promising biocompatible and biodegradable natural biomaterial, while glycerophosphate salts are well-known biocompatible agents; the formulations based on chitosan combinations can be held liquid at room temperature for encapsulating living cells and turn into hydrogel *in situ* at body temperature [5]. Immunohistochemistry clearly

Received March 20, 2011; accepted April 26, 2011

E-mail: biomater@mail.tsinghua.edu.cn (Q.L.F.), gzyubo@gmail.com (B.Y.)

* Co-first author

demonstrated that rat MSCs survived in the chitosan hydrogel for at least 28 d after injection in rats [4]. Using the chitosan hydrogel in humans, with an appropriate cell source or growth-factor/cell combination and controlled post-operative mobility, delivered cells could gradually produce a viable repair tissue at the defect site and thereby contribute to cell-based arthroscopic treatments for lesions of the articular cartilage [6]. However, chitosan do not promote osteogenesis of human MSCs cultured *in vitro* [7]. Ahmadi and colleagues [8] assessed the angiogenesis potential of chitosan cross-linked by hydroxyethyl cellulose for injectable bone tissue engineering applications; their results indicated that the chitosan crosslinked by cellulose did not induce angiogenesis, but the presence of human bone marrow-derived mesenchymal stem cells enhanced angiogenesis.

Bone tissues are mainly constructed from nano-sized hydroxyapatite (HA) minerals and type I collagen matrix with complex hierarchically assembled structures [9]. The ideal scaffolds for bone regeneration should promote early mineralization and support new bone formation [10]. Mineralized collagen fibrils (nHAC) composites seem to be very promising biomaterials for bone regeneration [11–13]. We previously developed a nHAC loaded chitosan injectable scaffold (CS/nHAC) with surface properties similar to physiological bone [14–15]. This composite (CS/nHAC) can be used to load MSCs *in vitro* homogeneously, injected into body in a minimally invasive manner, forms a non-decay hydrogel and provides a biocompatible environment for MSCs survival *in vivo* [16].

Bone marrow derived MSCs are present in adult bone marrow and are thought to be multipotent stem cells that can replicate as undifferentiated cells and have the potential to differentiate to lineages of mesenchymal tissues such as bone, cartilage, tendon, and marrow stroma [17]. Bone formation by bone marrow derived MSCs is dependent upon their transplantation with an appropriate scaffold [18]. In this study, we used CS/nHAC scaffold to encapsulate bone marrow derived MSCs (CS/nHAC/MSC) *in vitro* and co-injected the cell-matrix composites into a cancellous bone defects at the distal end of rabbit femurs [19–20]. The bone regeneration potential of the CS, CS/nHAC and CS/nHAC/MSC composites was reported.

2 Materials and methods

2.1 Materials

Medical grade chitosan was purchased from Shandong AK Biotech Ltd. (China). The molecular weight of chitosan estimated by size exclusion chromatography using dextran as standards was 2.5×10^5 Da and the degree of deacetylation of chitosan as determined by colloidal titration with polyvinyl sulfate potassium was 95.6%. Fetal bovine serum (FBS) was purchased from Hangzhou Sijiqing Biological Co., LTD. (China). Hydrated β-glycerophosphate disodium salt ($C_3H_7O_3PO_3Na_25H_2O$; M_w = 306) and Dulbecco's Modified Eagle's Medium (DMEM) were purchased from Sigma Chemical Co. (USA). All other reagents were of suitable analytical grade. nHAC is a composite biomaterial obtained by self-assembly of collagen triple helices [11]. Briefly, acid-soluble type I collagen was purchased from YierKang Company (China). The collagen was diluted to a concentration of 0.67 g collagen/L HCl (10 mmol/L) at 4ºC. $CaCl_2$ solution (14 mL, 0.1 mol/L) was added into 100 mL of collagen solution and maintained for 10 min. NaH_2PO_4 solution (8.4 mL, 0.1 mol/L) was added and the pH was adjusted to 7.0 by NaOH solution (100 mmol/L). The solution was maintained at pH 7.0 for 1 h, after which the composites were harvested by centrifugation at 5000 r/min (rpm). The composites were washed in deionized water and freeze-dried. The sterile water used in the experiments was triply distilled.

2.2 Methods

2.2.1 Allogeneic bone marrow derived MSCs isolation and culture expansion

Rabbit bone marrow were harvested from 3-week old New Zealand White rabbits under sterile conditions and the isolation and culture expansion of MSCs was performed according to previously published methods [21–22]. In brief, bone marrow was obtained from the femurs by flushing out with DMEM containing heparin (100 U/mL). Then the bone marrow was centrifuged at 1200 rpm for 5 min to obtain a cell pellet. Following removal of supernatant, cells were resuspended in Percoll gradient (1.083 g/mL) and centrifuged at 1200 g for 20 min. After being washed twice with DMEM, the cells were seeded at 5.0×10^6 cells/mL in low-glucose DMEM containing 10% FBS and cultured in a 5% CO_2 incubator at 37ºC. After 2 days, the culture medium was replaced and subsequently the medium was changed twice weekly. The adherent cells were allowed to reach approximately 80%–90% confluence. The third passage of the cells was used in this study.

2.2.2 Preparation of injectable hydrogel-forming solutions

The CS, CS/nHAC and CS/nHAC/MSC injectable hydrogel-forming solutions were prepared under sterile conditions. The CS injectable hydrogel-forming solution was prepared by the following procedure [23]. In short, chitosan solution was obtained by dissolving 2.2 g of chitosan in 100 mL of HCl solution (0.1 mol/L) and autoclave sterilized. Then 0.5 mL of $NaHCO_3$ solution (1 mol/L, sterilized by filtration) was added dropwise to the solution under stirring. To the resulting solution, the pH value of the solution was adjusted to 7.0 by adding droplets of β-glycerophosphate disodium salt solution [560 mg/mL, sterilized by filtration]. The CS/nHAC injectable hydrogel-forming solution was made by mixing 0.2 g nHAC with 9 mL chitosan solution. Then 0.5 mL of $NaHCO_3$ solution (1 mol/L, sterilized by filtration) was added dropwise to the solution under stirring. To the resulting solution, the pH of the solution was adjusted to 7.0 by adding droplets of β-glycerophosphate disodium salt solution [560 mg/mL, sterilized by filtration] [15]. For the CS/nHAC/MSC group, disc cells suspended in low-glucose DMEM containing 10% FBS were then added to the CS/nHAC solution (final cell density, 5×10^6 cells/mL). This solution was gently mixed to get a uniform suspension. The effect of cell density on the bone formation ability will be investigated in the future.

2.2.3 Surgery

The care and surgical procedure of the animals was approved by the Animal Care and Use Committee in Southern Medical University. Twenty four New Zealand White rabbits weighing 1.5–2.0 kg were used. General anaesthesia was induced with intravenous injection of 20% urethane (5 mL/kg). A lateral arthrotomy of the knee joint was performed and a cylindrical 7 mm × 10 mm osseous critical-sized defect was created at the distal femoral end (Fig. 1). In twelve rabbits, the right defects were injected with CS/nHAC/MSC and the left ones were injected with CS. In the remaining twelve rabbits, the right defects were injected with CS/nHAC and the left defects were untreated (untreated-group). The soft tissues were sutured in layers. Antibiotic therapy (penicillin, 8×10^5 U/day) was administered for 3 days after surgery. The animals were monitored postoperatively in the animal house until they were able to walk about. 4 ($n = 6$), 8 ($n = 6$), and 12 ($n = 12$) weeks after surgery, the animals were killed and the distal femurs were harvested, stripped of soft tissues, and fixed in 10% neutral formalin.

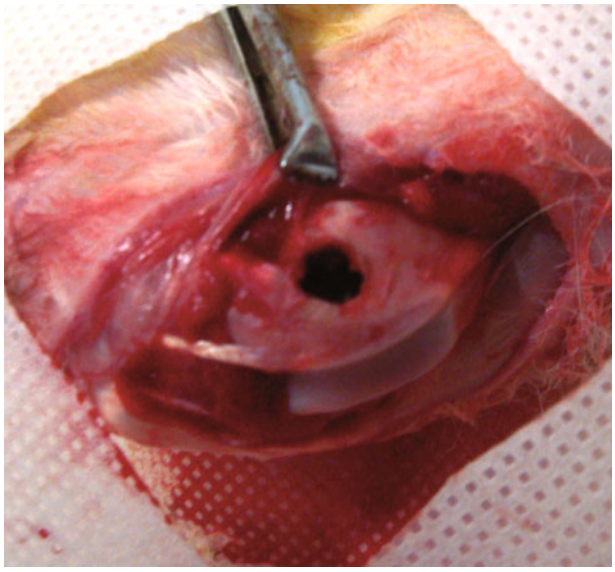

Fig. 1 Intraoperative view of a cylindrical 7 mm × 10 mm osseous critical-sized defect at the distal femoral end of the rabbit.

2.2.4 Measurement of bone density in the implantation site

Regeneration and remodeling of bone at the implantation site can be determined by trabecular bone density [24]. Helical Computed Tomography (CT) can now be combined with image processing to quantify trabecular bone density using CT Hounsfield units (HU) intensity [25–26]. In this study, the distal femurs were scanned on a Phillips CT scanner (Phillips/Brilliance 64, Phillips, Netherlands). Before scanning, calibration was performed according to the manufacturer's recommendations. The long axis of the femur was consistently aligned with the vertical axis of the scanner. The scan parameters were set at 120 kV, 150 mA·s, 0.5 s imaging time. A 3-cm image size, a 768 × 768 reconstruction matrix and a pitch factor of 0.579 were used. A bone algorithm was used, and the helical CT data were reconstructed at a 0.8 mm intervals and a slice thickness of 0.8 mm. All image data were processed using image analysis software (CT Viewer, Philips Medical Systems). For intensity measurements, a region of interest (ROI) was defined at the focus of the implanted area in all samples. A skilled pathologist determined the ROI area for each sample using PHILIPS Brilliance Workspace Version 3.5 (Philips Medical Systems, USA) software application. Most ROIs had at least 50 pixels within the identified region. The examiner measured the CT intensity of each

samples by calculating the average of all the CT HU gathered from three CT slices.

2.2.5 Micro-CT image acquisition

We used high-resolution micro-computed tomography (μCT) imaging to assess trabecular bone morphology [27]. A cone-beam μCT system developed by Institute of High Energy Physics (Chinese Academy of Sciences, China) was used. The long axis of the femur was consistently aligned with the vertical axis of the scanner. The femurs were scanned with X-ray source energy settings of 79 kV and 0.112 mA, resulting in a focal spot size of approximately 7 μm. The tomographies were performed on a range from 0º to 360°, in steps of 0.5°, resulting in 720 projections. The tomographic reconstructions were performed with locally written software based on the Feldkamp algorithm [28].

2.2.6 Histological preparation

The specimens used for histology were decalcified in buffered 10% EDTA and then embedded in paraffin. Tissue sections, 5 μm thick, were stained with hematoxylin and eosin (H&E) for morphologic analysis and Masson's trichrome for cross-linked collagen.

2.2.7 Raman microscopy

After Micro-CT scanning, the femoral extremities were sectioned along the long axis of the femur using a diamond saw to provide two halves of the implanted area. A HR800 Raman microscope (HORIRA Jobin-Yvon, France) fitted with a 10 mW, 633 nm laser and ×50/0.5 numerical aperture Achroplan immersion objective lens (OLYMPUS) was used to acquire spectra from the bone samples. At the beginning of each imaging session the laser was checked for alignment with the optical axis of the microscope and the wavenumber datum verified against a silicon standard. Data were recorded between 800 and 1200 cm^{-1} at a resolution of better than 1.6 cm^{-1}. Spectra were recorded from sites on engineered bone (CS/nHAC/MSC) and native bone. Each spectrum was the average of 10 accumulations each with a 10 s exposure time.

2.2.8 Statistical analysis

The bone density data between the CS, CS/nHAC, and CS/nHAC/MSC groups were compared using nonparametric Mann-Whitney U test. All analyses were performed using origin (version 8.0) statistical analysis software. A p-value of < 0.05 indicated statistical significance.

3 Results

Before bone sample retrieval, all the rabbits survived well and no operative or post-operative complications were encountered.

Figure 2 shows high resolution microradiographic images of untreated and injectable hydrogels-treated defects 12 weeks after operation. As expected, the defect did not spontaneously heal at 12 weeks (Fig. 2(a)). Bone trabecula progressively grew from the periphery of the cavity, and the highest percentage of bone regrowth was found in the CS/nHAC/MSC treated defect.

In Fig. 3, it was observed that the presence of nHAC in chitosan significantly ($p < 0.05$) increased the CT intensity of pure chitosan scaffolds at 8 and 12 weeks. Furthermore, by blending MSCs with the CS/nHAC, the CT intensity of CS/nHAC/MSC was significantly ($p < 0.05$) higher than CS/nHAC up to 12 weeks. Based on the averaged HU values, a statistically significant ($p < 0.05$) CT intensity increase in all cases was observed within the duration of implantation up to 12 weeks. The negative intensities in the untreated cavities indicated that the cavities were still filled with air or fat tissues. For the CS/nHAC/MSC group at 12 weeks, the intensity was (357±23) HU, indicating that calcified tissues might exist in the defect [24].

In the case of CS filler (Fig. 4), bone marrow was in close proximity of the undegraded chitosan. The degree of bone in-growth appeared to depend on the degradation of the chitosan. Fibrotic capsule was found around the undegraded chitosan even after 12 weeks. For the CS/nHAC group (Fig. 5), newly formed bone was in close proximity of the undegraded material core. The presence of newly formed bone around the undegraded matrixes indicated that the CS/nHAC matrixes promoted the in-growth of surrounding tissues. For the CS/nHAC/MSC group (Fig. 6), the cavity was mainly filled with new bone and collagen fibrous tissues. New bone was formed in the central implant area 12 weeks after implantation. Newly formed collagen bundles identified by Masson's trichrome stain were sparsely and unevenly distributed in the central implant area.

Raman spectra for the native bone and the newly formed bone (tissue engineered bone) of CS/nHAC/MSC group

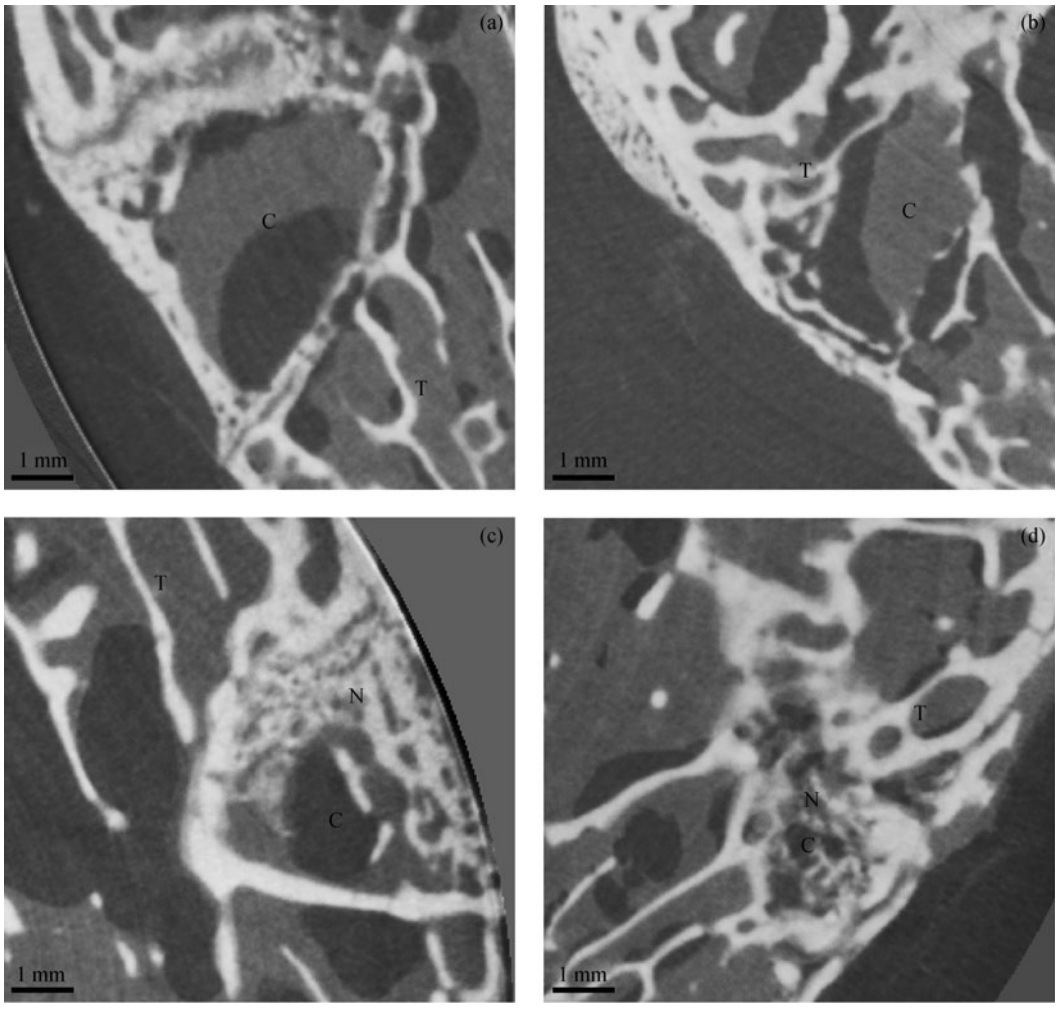

Fig. 2 High resolution μCT images in rabbit distal femur taken 12 weeks after implantation. **(a)** The untreated defect, the formation of new bone remains restricted to the edge of the cavity and the largest part of the centre of the cavity remains free of bone. **(b)** The chitosan treated defect, trabecula from the surrounding bone is growing towards the centre of the cavity, but the cavity is still visible. **(c)** The CS/nHAC treated defect, most of the cavity is occupied by new bone, but the central part of the cavity is still free of bone. **(d)** The CS/nHAC/MSC treated defect, trabecula from the surrounding bone is growing towards the centre of the cavity, and the central part of the cavity is occupied by new bone. (C: cavity; T: trabecula; N: new bone)

showed similar structural compositions (Fig. 7). The band at 961 cm^{-1} corresponded to the symmetric stretching vibration ($v1$) of the phosphate ion and was the strongest marker of bone mineral [29]. The intensity for the band at 961 cm^{-1} in the tissue engineered bone of CS/nHAC/MSC group was relatively low compared to the native bone, which indicated the relative low mineral content in the tissue engineered bone.

4 Discussion

The present study highlights the use of CS/nHAC composites as a new type of *in situ*-forming scaffold for bone repair as well as bone tissue engineering. The CS/nHAC solution was injected directly into cavities at the distal end of rabbit femurs and rapidly formed a stable gel *in situ*. As well, the CS/nHAC scaffolds were used to load MSCs homogeneously *in vitro* and injected into cavities in a minimally invasive manner to build a tissue engineered bone.

Chitosan alone was unable to directly stimulate the differentiation of MSCs to osteoblast or angiogenic factor release *in vitro*, which implied an indirect effect of chitosan on bone repair [7,23]. Other factors, such as an adequate repository of local stem cell pools surround the cavities at the distal end of rabbit femurs, and sufficient recruitment of

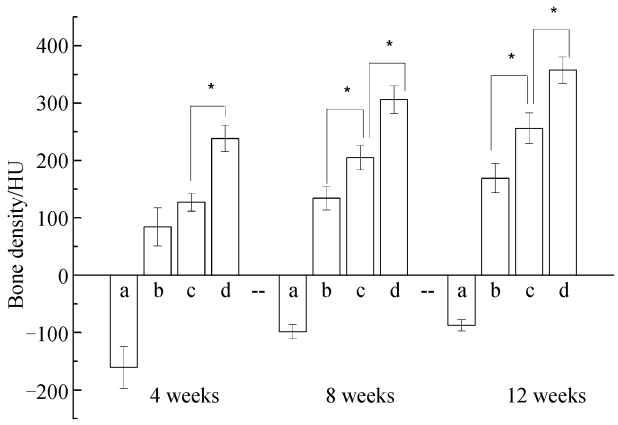

Fig. 3 Bone-mineral density measured in the implanted area, with Hounsfield units (HU) at 4, 8 and 12 weeks for each group (n = 3). (a —— untreated group; b —— CS group; c —— CS/nHAC group; d —— CS/nHAC/MSC group; ∗ —— $p < 0.05$)

specific cell types to the implantation site, were essential for bone formation of chitosan alone *in vivo* [23]. Our results using chitosan alone were consistent with them [7,23].

Our previous study confirmed that the CS/nHAC composites showed some features of natural bone both in main composition and microstructure to some extent. The inorganic phase is nano-sized carbonate-substituted HA with low crystallinity, and the small HA crystals associated with collagen fibrils show a preferred orientation of their *c*-crystallographic axis. The mineralized collagen fibrils aligned along their long axis as bundles. These bone-like features give the CS/nHAC composite itself bone-bonding ability [14]. In the present study, the surface of the CS/nHAC implant could provide a suitable environment for cell attachment, as well as collagen and bone mineral deposition. The histological analysis clearly showed that it led bone infiltration at the interface of the CS/nHAC matrixes and surrounding bone. However, the center of the defect was still unrepaired and some residual materials were evident for the CS/nHAC group after 12 weeks. These

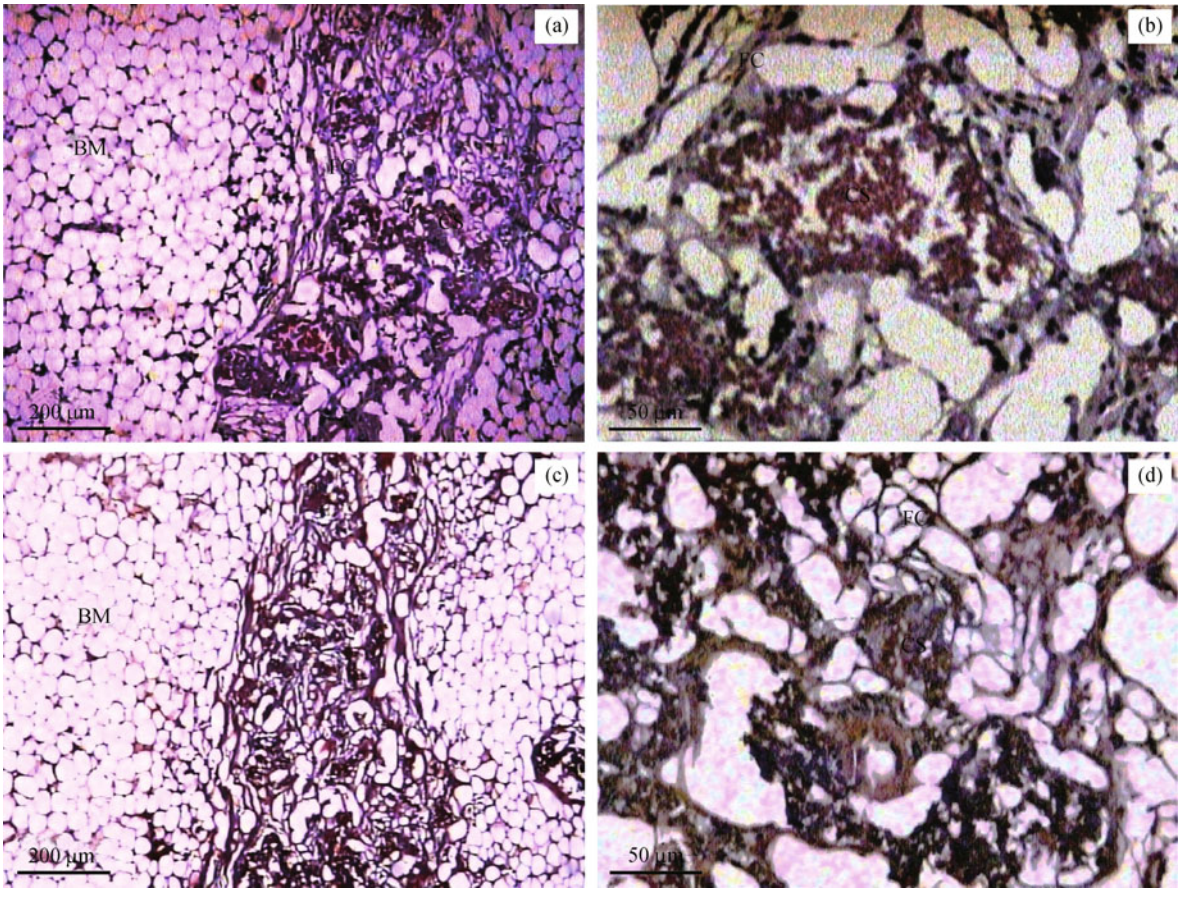

Fig. 4 Light microscopy photographs of the histology sections taken 12 weeks after implantation for CS group: **(a)** HE, 50×; **(b)** HE, 200×; **(c)** Masson, 50×; **(d)** Masson, 200×. (BM: bone marrow; CS: chitosan; FC: fibrotic capsule)

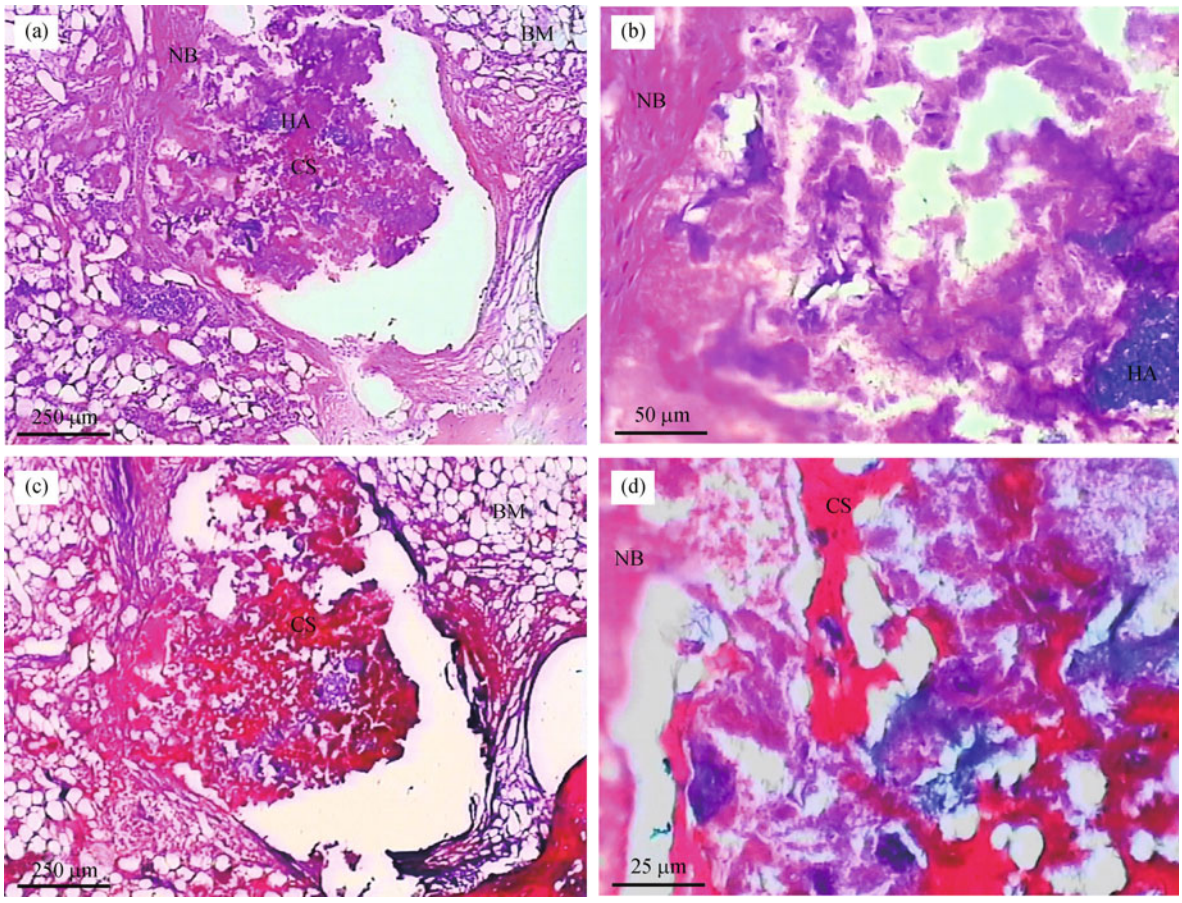

Fig. 5 Light microscopy photographs of the histology sections taken 12 weeks after implantation for CS/nHAC group: **(a)** HE, 40×; **(b)** HE, 200×; **(c)** Masson, 40×; **(d)** Masson, 400×. (NB: newly formed bone; BM: bone marrow; CS: chitosan; HA: nHAC)

experimental results indicated that using the CS/nHAC biomaterials alone was not effective to repair large bone defects, because the CS/nHAC biomaterials lack absorbability to recruit MSCs or osteogenic cells to the center of large defects.

Allogeneic MSCs are reported to survive after *in vivo* implantation [16] and modulate cellular immunity [30]. MSCs are also reported to be strong inducers of angiogenesis by attracting host-derived vascular endothelial cells through paracrine mechanisms with local release of arteriogenic cytokines [21,31]. Others have shown that uninduced MSCs were able to survive in the osteochondral defects and differentiate into osteoblasts, making a contribution to bone regeneration [32]. Studies using animal models have shown that MSCs are osteoinductive [33]. In this regard, we carried out the allogeneic MSCs implantation experiments using the injectable CS/nHAC scaffolds. We obtained MSCs from 3-week old New Zealand White rabbits. At 12 weeks after implantation, there were massive areas of new bone and collagen fibrous tissues in the center of the defects for the CS/nHAC/MSC group, confirming that the loaded MSCs not only enhanced osteoconduction of the CS/nHAC scaffolds but also might differentiate into osteoblasts, making a contribution to bone regeneration. However, the morphology of the tissue engineered bone was not similar to normal bone as revealed by histological investigations, and the mineral content of engineered bone was relatively low as revealed by Raman spectra. Further studies are needed to investigate whether the CS/nHAC/MSC composite could reconstitute the bone stock and structure in the longer term.

Tissue reactions to the chitosan implants were mild and characterized by fibrous connective tissue encapsulation. Hoemann et al. have found that chitosan hydrogels could guide macrophages to repairing sterile wounds *in vivo* [23]. Macrophages are also responsible for the degradation of chitosan *in vivo* through the release of several cytokines such as tumor necrosis factor-α and interleukin-1β, which attract fibroblasts into the wound to initiate the reconstruction process [34]. nHAC could be easily resorbed by cells

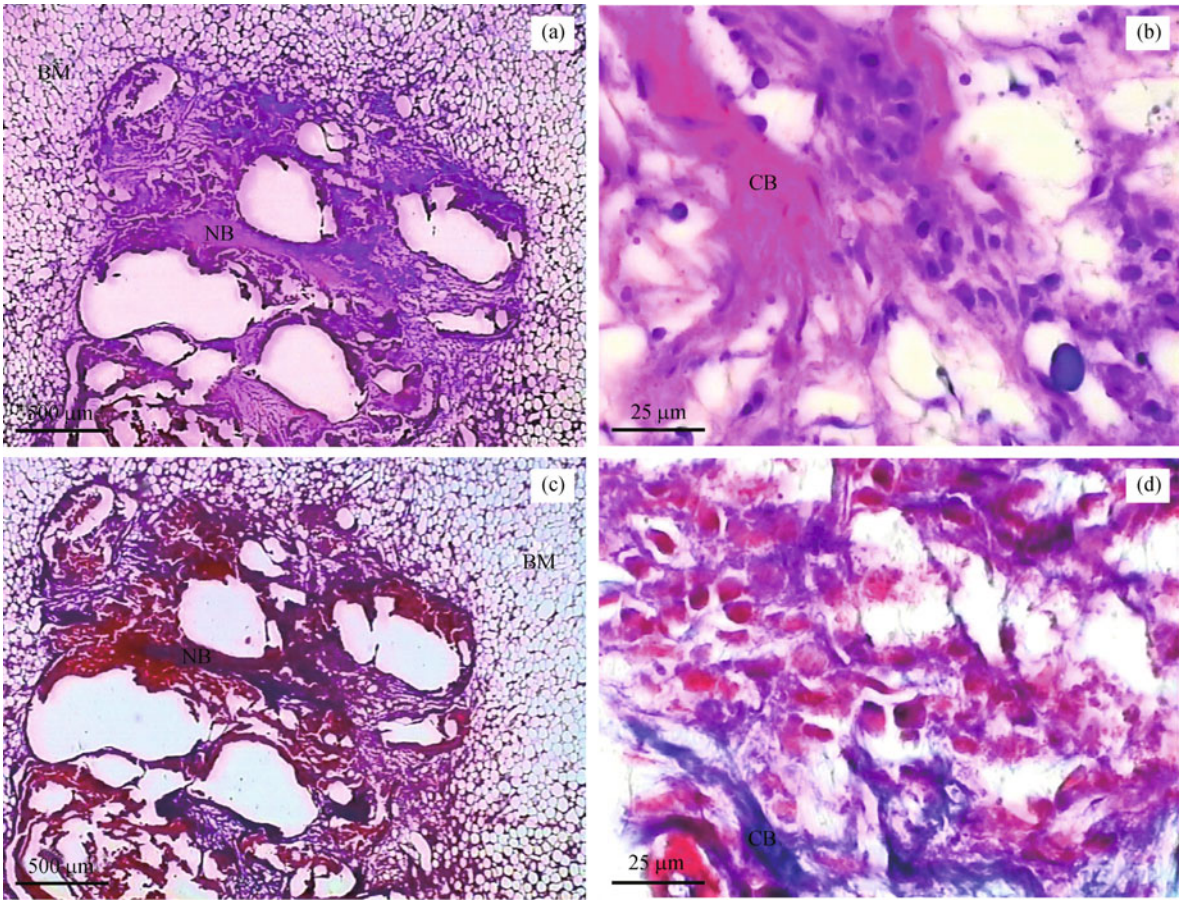

Fig. 6 Light microscopy photographs of the histology sections taken 12 weeks after implantation for the CS/nHAC/MSC group: **(a)** HE, 20×; **(b)** HE, 400×; **(c)** Masson, 20×; **(d)** Masson, 400×. (NB: newly formed bone; BM: bone marrow; CB: collagen bundles)

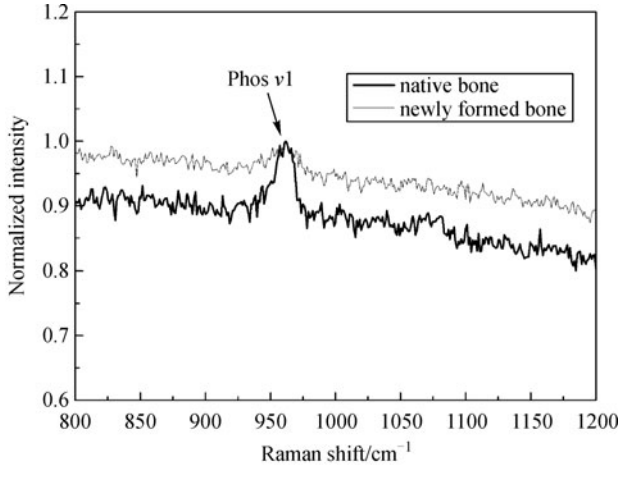

Fig. 7 Raman spectra for the native bone and newly formed bone in the CS/nHAC/MSC group.

because it was made of HA nanocrystals and collagen nanofibrils and has porous bone-like structure [11,35]. It previously showed that the degradation rate of nHAC was the same as the formation rate of new bone by providing initial mechanical support and directing the growth of osteoblasts [36–37]. No fibrotic capsule was found in the CS/nHAC/MSC filled defects. MSCs have been suggested to lower the risk of both acute and chronic graft-versus host disease after allogeneic stem cell transplantation [38–39]. The excellent biocompatibility of CS/nHAC/MSC and enhanced new bone formation *in vivo*, as revealed by the histological results, may be in part due to the immune privileged properties of MSCs.

5 Conclusions

A new injectable bone graft material with osteogenic capacity was made by the CS/nHAC scaffolds seeded with MSCs. This composite scaffold could load MSCs homogeneously *in vitro* and injected into cavities directly in a minimally invasive manner to build a tissue engineered bone *in situ*. Massive areas of new bone and collagen fibrous tissues formed in the center of the defects after 12 weeks. The results of present study showed that the

CS/nHAC/MSC composite was a novel injectable bone graft substitute to repair a large bone defect effectively.

Acknowledgements The authors are grateful for the financial support from the 973 Project (2007CB815604), National Natural Science Foundation of China (51072090, 51061130554), Natural Science Foundation of Guangdong Province, China (10451051501004727) and Doctor Subject Foundation of the Ministry of Education of China (20100002110074).

References

[1] Sittinger M, Hutmacher D W, Risbud M V. Current strategies for cell delivery in cartilage and bone regeneration. Current Opinion in Biotechnology, 2004, 15(5): 411–418

[2] Hou Q P, De Bank P A, Shakesheff K M. Injectable scaffolds for tissue regeneration. Journal of Materials Chemistry, 2004, 14(13): 1915–1923

[3] Kretlow J D, Young S, Klouda L, et al. Injectable biomaterials for regenerating complex craniofacial tissues. Advanced Materials, 2009, 21(32–33): 3368–3393

[4] Cho M H, Kim K S, Ahn H H, et al. Chitosan gel as an *in situ*-forming scaffold for rat bone marrow mesenchymal stem cells *in vivo*. Tissue Engineering Part A, 2008, 14(6): 1099–1108

[5] Chenite A, Chaput C, Wang D, et al. Novel injectable neutral solutions of chitosan form biodegradable gels *in situ*. Biomaterials, 2000, 21(21): 2155–2161

[6] Hoemann C D, Sun J, Legare A, et al. Tissue engineering of cartilage using an injectable and adhesive chitosan-based cell-delivery vehicle. Osteoarthritis and Cartilage, 2005, 13(4): 318–329

[7] Guzman-Morales J, El-Gabalawy H, Pham M H, et al. Effect of chitosan particles and dexamethasone on human bone marrow stromal cell osteogenesis and angiogenic factor secretion. Bone, 2009, 45(4): 617–626

[8] Ahmadi R, Burns A J, de Bruijn J D. Chitosan-based hydrogels do not induce angiogenesis. Journal of Tissue Engineering and Regenerative Medicine, 2010, 4(4): 309–315

[9] Olszta M J, Cheng X G, Jee S S, et al. Bone structure and formation: A new perspective. Materials Science and Engineering R: Reports, 2007, 58(3–5): 77–116

[10] Cui F Z, Li Y, Ge J. Self-assembly of mineralized collagen composites. Materials Science and Engineering R: Reports, 2007, 57(1–6): 1–27

[11] Zhang W, Liao S S, Cui F Z. Hierarchical self-assembly of nano-fibrils in mineralized collagen. Chemistry of Materials, 2003, 15 (16): 3221–3226

[12] Liao S S, Guan K, Cui F Z, et al. Lumbar spinal fusion with a mineralized collagen matrix and rhBMP-2 in a rabbit model. Spine, 2003, 28(17): 1954–1960

[13] Li X M, Feng Q L, Jiao Y F, et al. Collagen-based scaffolds reinforced by chitosan fibres for bone tissue engineering. Polymer International, 2005, 54(7): 1034–1040

[14] Huang Z, Feng Q, Yu B, et al. Biomimetic properties of an injectable chitosan/nano-hydroxyapatite/collagen composite. Materials Science and Engineering C, 2011, 31(3): 683–687

[15] Huang Z, Tian J, Yu B, et al. A bone-like nano-hydroxyapatite/collagen loaded injectable scaffold. Biomedical Materials, 2009, 4 (5): 055005 (7 pages)

[16] Huang Z, Yu B, Feng Q, et al. *In situ*-forming chitosan/nano-hydroxyapatite/collagen gel for the delivery of bone marrow mesenchymal stem cells. Carbohydrate Polymers, 2011, 85(1): 261–267

[17] Pittenger M F, Mackay a M, Beck S C, et al. Multilineage potential of adult human mesenchymal stem cells. Science, 1999, 284 (5411): 143–147

[18] Mankani M H, Kuznetsov S A, Wolfe R M, et al. *In vivo* bone formation by human bone marrow stromal cells: Reconstruction of the mouse calvarium and mandible. Stem Cells, 2006, 24(9): 2140–2149

[19] Gauthier O, Muller R, Von Stechow D, et al. *In vivo* bone regeneration with injectable calcium phosphate biomaterial: A three-dimensional micro-computed tomographic, biomechanical and SEM study. Biomaterials, 2005, 26(27): 5444–5453

[20] Giavaresi G, Fini M, Salvage J, et al. Bone regeneration potential of a soybean-based filler: experimental study in a rabbit cancellous bone defects. Journal of Materials Science: Materials in Medicine, 2010, 21(2): 615–626

[21] Yoon S J, Park K S, Kim M S, et al. Repair of diaphyseal bone defects with calcitriol-loaded PLGA scaffolds and marrow stromal cells. Tissue Engineering, 2007, 13(5): 1125–1133

[22] Kasten P, Vogel J, Geiger F, et al. The effect of platelet-rich plasma on healing in critical-size long-bone defects. Biomaterials, 2008, 29(29): 3983–3992

[23] Hoemann C D, Chen G P, Marchand C, et al. Scaffold-guided subchondral bone repair implication of neutrophils and alternatively activated arginase-1 + macrophages. The American Journal of Sports Medicine, 2010, 38(9): 1845–1856

[24] de Oliveira R C G, Leles C R, Normanha L M, et al. Assessments of trabecular bone density at implant sites on CT images. Oral Surgery Oral Medicine Oral Pathology Oral Radiology and Endodontology, 2008, 105(2): 231–238

[25] Kobayashi F, Ito J, Hayashi T, et al. A study of volumetric visualization and quantitative evaluation of bone trabeculae in helical CT. Dentomaxillofacial Radiology, 2003, 32(3): 181–185

[26] Shinbo J, Mainil-Varlet P, Watanabe A, et al. Evaluation of early tissue reactions after lumbar intertransverse process fusion using CT in a rabbit. Skeletal Radiology, 2010, 39(4): 369–373

[27] Bouxsein M L, Boyd S K, Christiansen B A, et al. Guidelines for assessment of bone microstructure in rodents using micro-computed tomography. Journal of Bone and Mineral Research, 2010, 25(7): 1468–1486

[28] Feldkamp L A, Davis L C, Kress J W. Practical cone-beam algorithm. Journal of the Optical Society of America A: Optics, Image Science, and Vision, 1984, 1(6): 612–619

[29] Goodyear S R, Gibson L R, Skakle J M S, et al. A comparison of cortical and trabecular bone from C57 Black 6 mice using Raman spectroscopy. Bone, 2009, 44(5): 899–907

[30] Aggarwal S, Pittenger M F. Human mesenchymal stem cells modulate allogeneic immune cell responses. Blood, 2005, 105(4): 1815–1822

[31] Kinnaird T, Stabile E, Burnett M S, et al. Local delivery of marrow-derived stromal cells augments collateral perfusion through paracrine mechanisms. Circulation, 2004, 109(12): 1543–1549

[32] Tatebe M, Nakamura R, Kagami H, et al. Differentiation of transplanted mesenchymal stem cells in a large osteochondral defect in rabbit. Cytotherapy, 2005, 7(6): 520–530

[33] Korda M, Hua J, Little N J, et al. The effect of mesenchymal stromal cells on the osseoinduction of impaction grafts. Tissue Engineering Part A, 2010, 16(2): 675–683

[34] Chellat F, Tabrizian M, Dumitriu S, et al. *In vitro* and *in vivo* biocompatibility of chitosan-xanthan polyionic complex. Journal of Biomedical Materials Research, 2000, 51(1): 107–116

[35] Liao S S, Cui F Z. *In vitro* and *in vivo* degradation of mineralized collagen-based composite scaffold: Nanohydroxyapatite/collagen/poly(L-lactide). Tissue Engineering, 2004, 10(1–2): 73–80

[36] Li X M, Feng Q L, Liu X H, et al. Collagen-based implants reinforced by chitin fibres in a goat shank bone defect model. Biomaterials, 2006, 27(9): 1917–1923

[37] Li X M, Liu X H, Zhang G P, et al. Repairing 25 mm bone defect using fibres reinforced scaffolds as well as autograft bone. Bone, 2008, 43(suppl 1): S94

[38] Frassoni F, Labopin M, Bacigalupo A, et al. Expanded mesenchymal stem cells (MSC), co-infused with HLA identical hemopoietic stem cell transplants, reduce acute and chronic graft versus host disease: A matched pair analysis. Bone Marrow Transplantation, 2002, 29(suppl 2): S2

[39] Rasmusson I, Ringden O, Sundberg B, et al. Mesenchymal stem cells inhibit lymphocyte proliferation by mitogens and alloantigens by different mechanisms. Experimental Cell Research, 2005, 305(1): 33–41